ACADEMIA ROMÂNĂ
Revue Roumaine de Chimie
http://web.icf.ro/rrch/

Rev. Roum. Chim.,
2021, *66*(7), 613–624
DOI: 10.33224/rrch.2021.66.7.04

ENHANCEMENT OF THE PHOTODEGRADATION RESISTANCE AND ANTIBACTERIAL PROPERTIES OF PP-HDPE NANOCOMPOSITES BASED NANOCLAY AND ZINC OXIDE

Hicham KOUADRI,[a,b*] Ouahiba BOURICHE,[a,b,*] Ouarda DJAOUT,[b] Naima MAOUCHE[c] and Djahida LERARI[a,d]

[a] Center for Scientific and Technical Research in Physico-chemical Analysis (CRAPC), BP 384, zone Industrielle Bou-Ismail RP 42004 Bou Ismaïl, Tipaza, Algeria
[b]Department of Process Engineering, University of Ferhat Abbas Setif-1 19000, Algeria
[c]Laboratory of Electrochemistry and Materials (LEM), Department of Process Engineering, University of Ferhat Abbas Setif-1 19000, Algeria
[d] Laboratory of Macromolecular and Macromolecular Thio-organic Synthesis, Faculty of Chemistry, U.S.T.H.B., B.P. 32 El-alia Bab-ezzouar, 16111 Algiers, Algeria

Received May 27, 2020

A new series of polypropylene/high density polyethylene nanocomposites based on clay and zinc oxides (PP-HDPE/clay-ZnO) with different contents of nano-fillers (1%wt, 3%wt, 5%wt) were prepared by melt blending process in the presence of dicumyl peroxide (DCP) as a free radical generator and maleic anhydrides (MAH) as across linking agents. In this work, the Zinc oxide nanoparticles (ZnO) were added to increase resistance to ultraviolet light, and antimicrobial activity of nanocomposite films. The attachment and anchoring of ZnO nanoparticles to the surface of clay minerals can provide more active surface positions, reduce the agglomeration of nanoparticles and prevent their release into the environment that would result in poor toxicity and would ensure antibacterial activity over time.The morphological (DRA), structures, a rheological, thermal, photocatalytic, and antibacterial properties of the composite films were investigated as a function of clay and ZnO content. The Dynamical a rheological analysis DRA results showed that binary blends based on PP-HDPE, as deduced from the torque - time curves exhibit cross-linking reactions. This has taken place in the molten state after polymer fusion. And the evaluation of T_B equilibrium showed that the crosslinking effect starts to be apparent and given the highest value in the sample (PP-HDPE$_G$ /oMt-ZnO5).The XRD spectra show the absence of the characteristic peaks of clay in the formulation which contains modified montmorillonite in the presence of ZnO, this may be due to the exfoliated structure in the nanocomposite matrix. The photodegradation of various formulations have shown that there is no oxidation of the polymers composites in the presence of ZnO. The antibacterial efficacy of the composites varied with the dispersion, and the content of the ZnO particles. It is noted that the antibacterial effect was present altogether the formulations containing ZnO, and maximum inhibition of bacterial growth was observed in PP-HDPE$_G$/oMt-ZnO3, and PP-HDPE$_G$ /oMt-ZnO5 composites with Escherichia coli, this is due to the higher content of ZnO, activated surface area and better dispersion resulting by the attachment of ZnO nanoparticles to the surface of modified montmorillonite (o-Mt). Hence, these materials with good anti UV resistance and antibacterial activity are looked for. Such it can find them applications in hospitals spaces mainly operating rooms, laboratories, and health equipment mostly in the pandimics period.

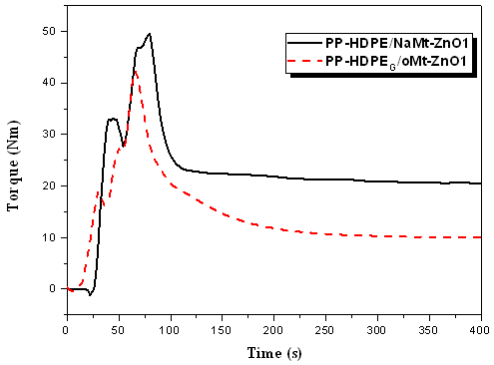

INTRODUCTION

In the past few months, the worldwide spread of the COVID-19 pandemic has been worrying. According to the recommendations of the World Health Organization (WHO), this pandemic has greatly increased the use and production of masks and other components (gloves, face shields,

* Corresponding authors: chinpolyhim@yahoo.fr; kouadri.hicham@crapc.dz or anesk2011@yahoo.fr; bouriche.ouahiba@crapc.dz

protective clothing, and safety shoes) made with polymeric materials[1]. Bacterial contamination on the surface is a major problem in many fields, such as the medical or food industry. Antimicrobial polymers are emerging new disinfectants, and in some cases can even be used as substitutes for antibiotics. Interestingly, the antimicrobial polymer can be bound to the surface without losing its biological activity, which allows the design of a surface that can kill microorganisms without releasing biocides[2]. Researchers from different institutes have developed antimicrobial and antibacterial polymers. These polymers could be used for example in the medical field, for food packaging, in air filters, and in all areas, including common places, close doors, and work tables. Researchers are looking to continue the development of these polymers to extend them to membranes or textiles.[1, 3-8] In addition, compared to ordinary nanomaterials, the support of nano-sized semiconductor materials on the substrate can help to enhance their activity. In this regard, various clay matrices such as kaolinite, montmorillonite and bentonitehavebeen successfully used assupports. Kaolinite has special crystalline chemical characteristics. Therefore, it can be used as a suitable substrate for anchoring ZnO nanoparticles.[9,10-18] Fixing and anchoring nano-sized ZnO nanoparticles on the surface of clay minerals can provide more active surface positions, reduce the agglomeration of nanoparticles, and prevent the release of nanoparticles into the environment. Artificial polymeric clay nanocomposites have become the main focus of research and metallic nanoparticles have been studied in the latest research results to study environmental pollutants. Because ZnO nanoparticles are cheap, non-toxic and can remove emerging pollutants, and considering that rural communities are affected by wastewater pollutants. However, as a functional inorganic filler, nano-scale zinc oxide (ZnO) has been widely used in functional equipment, catalysts, pigments, optical materials, cosmetics, ultraviolet absorbers and additives in many industrial products. Several reports have been published on the antibacterial activity of ZnO in polymer matrix.[11-20] To the best of our knowledge, there have been no reports on PP-HDPE/o-Mt-ZnO nanocomposite films and their properties for use as packaging, and as medical equipment materials antibacterial. In this work, six different nanocomposite films were prepared by melt mixing, and the effects of the clay and ZnO content on the arheological, morphological, structure, thermal, and antibacterial properties of the films were investigated. Although, the studies on clay nanocomposites based on PP/PE blends, using different compatibilizers, are not very numerous. Among the work of Parameswaranpillaiand his colleagues,[21] in which, they report that the presence of EPDM in PP/HDPE (80/20) blends enhanced the impact strength and elongation at break, but at the expense of tensile strength and modulus. The morphology of the ternary composite material reveals the complex morphology of interpenetration. The presence of xGnP in the ternary blend greatly improves the tensile toughness of the composite material. The storage modulus and loss modulus of PP/HDPE blends are reduced by adding EPDM elastomer. The PE-MAH played a better compatibilizer role. The effects of adding organophilic montmorillonite (o-MMT) and/or ethylene propylene diene monomer (EPDM)-MAH on the phase morphology, the thermal and mechanical properties of the PP/ HDPE blends have investigated by several researchers.[8,22,23] Adding EPDM-MAH to PP/HDPE/o-MMT blends will reduce tensile strength and flexural modulus/strength. However, the impact strength notably increased. It is well established that inorganic particles (ZnO, o-MMT) not only increase the mechanical strength of the polymers, but can also provide antibacterial property and ultraviolet resistance.[8,23]

EXPERIMENTAL

1. Materials

Commercial polypropylene (PP) (Sabic-500P, soften Flow index at 230°C and 2.16 kg; 3g/10 min. Density D= 792) and polyethylene high density (HDPE) (Sabic-F00952, soften flow index at 190 °C and 2.16 kg; 0.05g/10 min, D= 952 kg/ m³) were used as received. The reagents: dicumyl peroxide (DCP, Bayer ltd), maleic anhydride (MAH, Sigma-Aldrich), benzyl tributyl ammonium chloride (BTBA, Flukapurum>98%), and zinc oxide nanoparticles (ZnO rutile 99.9%, Sigma-Aldrich) were used without further purification. The clay mineral from Maghnia was kindly supplied by ENOF (Algiers, Algeria). Lamp UV 32wat (λ 300-400 nm) distance at 20 cm.

2. Clay organomodification

Before organomodification, the mono-ionized step was firstly conducted, as follows: 100 g of natural bentonite clay (NaMt) were dispersed in sodium chloride (NaCl) solution (1N), is brought into contact in 1 L of a NaCl solution (1M) and the suspension was stirred for 24h. This operation was repeated three times. The obtained suspension was washed with distilled water several times, until the chloride ions completely disappeared. After sedimentation, the suspension was centrifuged, dried, and the solid was finally crushed. The sodic clay was dispersed a hot aqueous solution (80°C) containing 10^{-2} moles of the benzyl tributyl ammonium chloride and the suspension was stirred for 3 h, then washed several times with distilled water at 60°C. The obtained organophilic clay, noted oMt was dried for 36h, crushed, sieved and stored.[8,23]

Table 1

Description of the studied (nano)composites

(Nano)composite	Polymers		Clays		Oxide	Compatibilizer
	PP	HDPE	NaMt	oMt	ZnO	MAH
PP-HDPE/NaMt-ZnO1	50	50	1	-	1	-
PP-HDPE/NaMt-ZnO3	50	50	3	-	3	-
PP-HDPE/NaMt-ZnO5	50	50	5	-	5	-
PP-HDPE$_G$/oMt-ZnO1	50	50	-	1	1	1
PP-HDPE$_G$/oMt-ZnO3	50	50	-	3	3	3
PP-HDPE$_G$/oMt-ZnO5	50	50	-	5	5	5

3. Nanocomposites preparation

Nanocomposites based on PP and HDPE blend (50:50) were prepared using clay (NaMt or oMt), as nanofillers and ZnO nanoparticles. The composites were prepared by melt blending using a Hake Record Plastograph (Cergy-ontoise, France), operating at 180°C for 10 min, with a rotation speed of 30 rpm. The obtained composites were compression-molded at 180°C under a pressure of 5MPA and then cooled to room temperature. In order to improve the UV resistance of zinc oxide nanoparticles, samples were exposed to ultraviolet light radiations for 120 h, using UV lamp (32 W). the distance sample-UV source was 20 cm, under air atmosphere, at room temperature. Table 1 summarizes the composition of all formulations.

4. Antibacterial tests

The antibacterial properties of the obtained nanocomposites were evaluated using the counting viable cells technique (JIS Z 2801), by examining their ability to kill Escherichia coli (E. Coli). For this, the plates were, firstly, disinfected with ethanol, and then exposed to the UV irradiations (Vilber Lourmat, VL 6), in the wavelength range of 300-400 nm, for 2 h. Then, 50 µL of the solution containing E.Coli of 105 colony-forming units were dropped onto the composite plates and the composites films were used to cover the specimen shaving Luria Bertani (LB) agar. The formulations were cultured at 37 ° C for 24 h. Then, films were washed in sterile 0.9% NaCl solution. The surviving bacteria was evaluated using spread plate method. The distinction of viable live cell variation of recognizing materials PP-HDPE / NaMt-ZnO (1%wt, 3%wt, 5%wt) and (PP-HDPE$_G$/oMt-ZnO) (1%wt, 3%wt, 5%wt) is obtained by comparing the reduction in the index of viable cells on the culture discs.[10]

5. Characterization

X-ray diffraction (XRD) measurements were conducted using PANanalyticalX'PertPro diffractomer, with monochromatic CuKα radiation, at a wavelength λ of 1.5418Å, at an accelerating voltage of 40kV and an electrical current of 45 mA. The data were collected from 1.65° to 30° by step of 0.04° and scanning rate of 0.6°.min^{-1}. Fourier Transform Infrared (FTIR) spectra with Attenuated Total Reflectance mode (FTIR-ATR) were performed on a spectrophotometer Bruker Vector 22 Spectrometer GmbH, in the frequency range of 4000–400cm^{-1},with an accumulation of 32 scans and are solution of 4cm^{-1}. Thin films (micronthick) were obtained by hotpressing. The thermogravimetric analysis was carried out using an "SDT Q600" device "TA Instruments". The samples witch characterized were subjected to a temperature ramp from 50°C to 600°C. The speed of the temperature ramp is 0.2°C/s under a flow of nitrogen. Differential Scanning Calorimetry (DSC) analyses were performed according to a Mettler Toledo Star System 30. (Nano)composites (~ 15 mg) were sealed in aluminium pans for analysis according to the following program: samples were heated from 25°C to 200°C, with a heating rate of 10°C min^{-1}, under nitrogen atmosphere. Relevant data were collected from the second heating scan.

RESULTS AND DISCUSSION

1. Dynamical rheological analysis (DRA)

Analysis of the torque-time evolution during the melt blending of all materials reveals resulting cross-linking reactions of various components. Figure 1 illustrates the evolution of all systems during compounding. From the plot of torque as a function of time, it is often seen that originally, the polymers Melts, and also the force decreases to a minimum price that describes the transformation from the solid to the molten state (point T_A). In our case, we have two breasts T_A due to the melting point of the two polymers PP and HDPE.[8,23] When the cross-linking reaction begins, the torsion will increase till reaching the utmost worth (point T_B). After which, a partial decrease of the torque is observed. This slight decrease is attributed to the partial destruction of the network already formed being even lower in the presence of peroxide. This is due to the attack by the peroxide radicals (particularly at the tertiary carbons of PP, which are the more reactive sites), to form macro radicals by disproportionately or by cyclization of the end groups, which is, mainly attributed to the fact that PP degradation, in the presence of peroxide, results in shorter chains through session reactions. This means that the viscosity will diminish, owing to the decrease in the molecular weight. These results have already been reported by Mirigul Altan et al on polypropylene with peroxide.[24] Where an increase in the torque values was observed. This was an indication that cross linking reactions occurred, originating a molecular weight increase (Figure 1). The evaluation of T_B at the equilibrium shows that the crosslinking effect starts to be apparent from (PP/HDPE$_G$/oMt-ZnO 5). This positive deviation is proportional to the degree of crosslinking in the matrix. As mentioned antecedently, the formation of a complex network takes place, and therefore, the evolution of the torsion is plagued by the PP degradation However, the presence of ZnO has no apparent effect on the torque-time evolution.

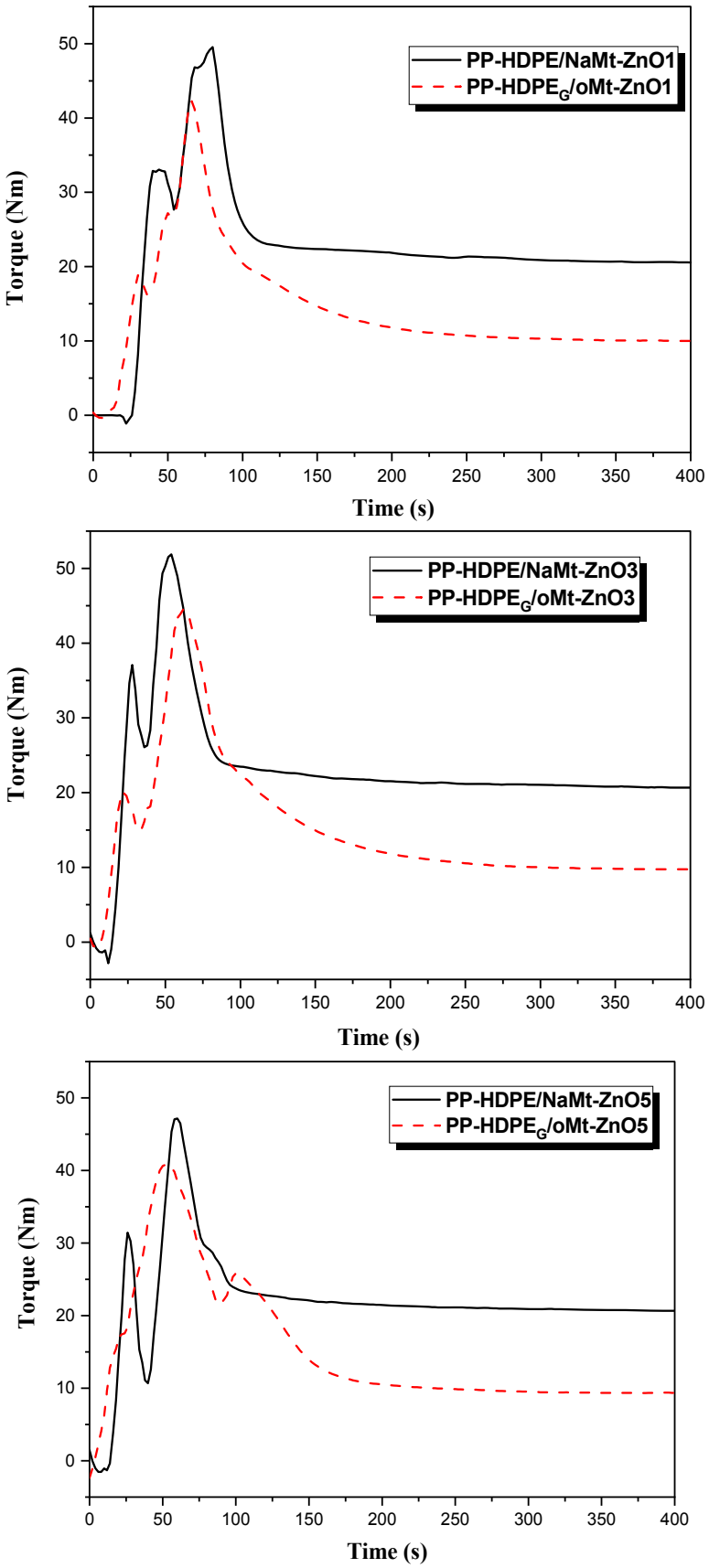

Fig. 1 – Evolution of the torque versus time during melt compounding of the PP-HDPE/clay-ZnO nanocomposites (60 rpm and 180°C).

2. Nanocomposites structure

The organomodification of the montmorillonite was evaluated according to Bragg's equation $n\lambda = 2d \sin\theta$ based on XRD results. As shown in Figure 2, the pristine clay has an interlayer spacing d_{001}= 12.6 Å (2θ = 7.05°). After organomodification, the d_{001} value shifts to 17.7Å (2θ = 5.04°). This spacing increase is in indication of the efficient of the organomodifier intercalation. The XRD patterns of PP-HDPE (nano)composites with different percent of clay (unmodified or modified) and zinc oxide are presented in Figures 3 and 4, respectively. The systems based on the unmodified clay (PP-HDPE/NaMt-ZnO) show a diffraction peak around 2θ =5°, attesting the formation of an intercalated structure (Figure 3). In the case of PP-HDPE$_G$/oMt-ZnO1, PP-HDPE$_G$/oMt-ZnO3 and PP-HDPE$_G$/oMt-ZnO5, no diffraction peak was detected at low 2θ angle. This result is an indication of a total delamination of the clay platelets and hence the formation of exfoliated nanocomposites (Figure 4).

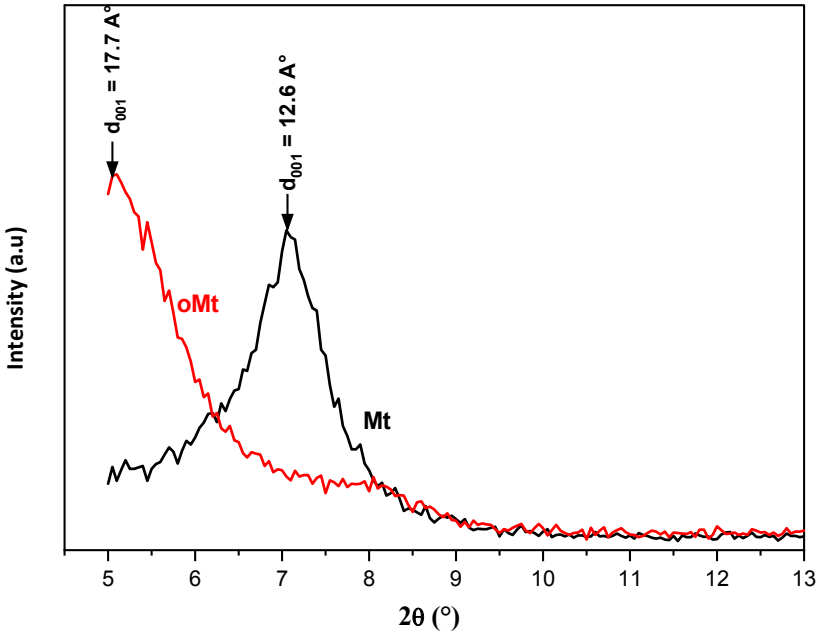

Fig. 2 – XRD patterns of clay before and after organomodification.

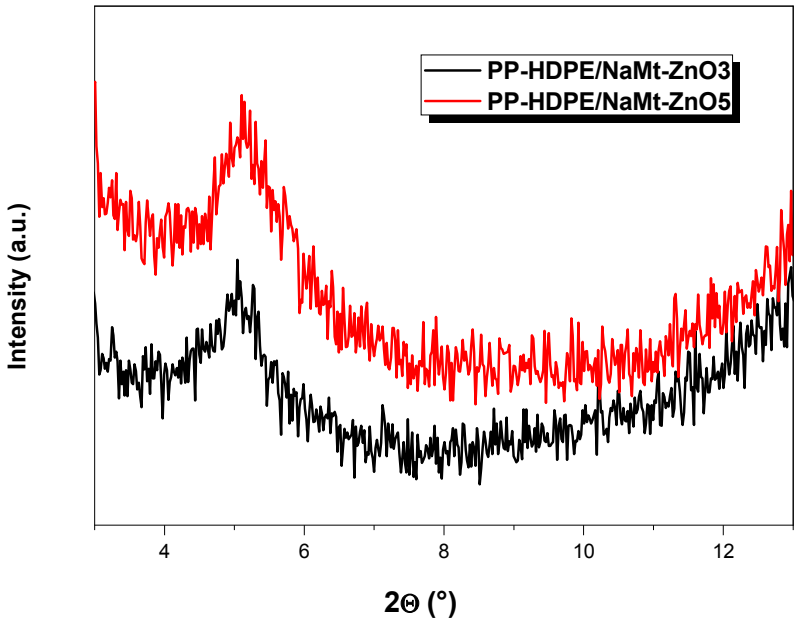

Fig. 3 – XRD patterns of PP-HDPE/NaMt-ZnO nanocomposites.

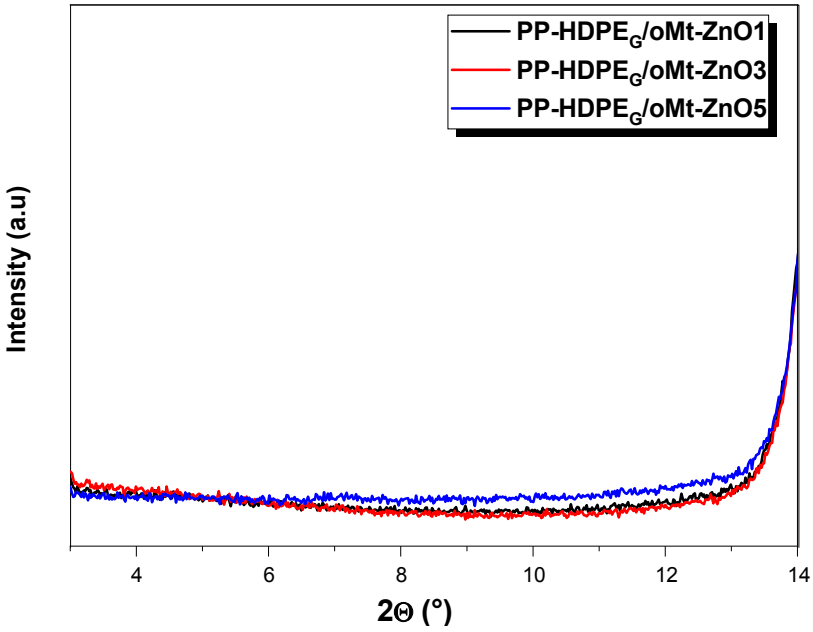

Fig. 4 – XRD patterns of PP-HDPE/oMt-ZnO nanocomposites.

3. Thermal properties

Generally, the formation of the exfoliated structure of polymers nanocomposites based on organomodified clays involves an enhancement on the thermal properties of the system as compared to that based on unmodified clays. In order to underline this effect of clay nature on the PP-HDPE thermal stability, TGA analyses were performed under air flow, with a heating rate of 20°C min^{-1}. Figures 5 and 6 show the TGA/DTG curves of PP-HDPE/NaMt-ZnO and PP-HDPE$_G$/oMt-ZnO, respectively. The peak assigned to the scission of the C-C chemical bond of the PP-HDPE polymer shifted to higher temperature in the case of oMt nano-filler as compared to NaMt. For exemple, the DTG maximum shifted from 455°C for PP-HDPE/NaMt-ZnO1 to 467°C for PP-HDPE$_G$/oMt-ZnO1, implying an improvement of the thermal stability by about 12°C. Comparable enhancement is detected with the other formulations (Table 2). The organomodified clay displays a better dispersion on the PP-HDPE and underlines, hence, an efficient barrier effect that restricts the diffusion of oxygen toward the polymer matrix, as compared to unmodified one. However, the DSC results of nanocomposites presented in Figures 7a and 7b show two melting temperature (Tm). The first around 140°C, relied to the HDPE and the second at 160°C, attributed to the PP. The values of these temperatures are slightly affected by the presence of clay nanofiller and ZnO nanoparticles (Not exceed 4°C, inall cases). In addition, according to the Tm values, it can be said there is an effect on the crystallization mode of each crystalline part of the mixtures. This is due to the fact that when PP starts to crystallize, HDPE is still in the molten state, and this will affect the nucleation rate of the PP. On the other hand, when HDPE starts to crystallize, the PP is in a solid state and this will then affect the growing rate of HDPE. Therefore, as a result, these two modes are related to chain dispersion.[8,23-27]

4. Ultraviolet degradation resistance

In order to underline the effect ZnO nanoparticle to prevent the nanocomposites photo-degradation, these later were exposed to UV irradiations for 300 h ours and the FTIR spectra were compared to the PP-HDPE/NaMt blend after UV exposure. Figures 8a and 8b depict the infrared spectra of the different formulations, in the range of carbonyl group, resulting from the photo-degradation reaction of alkyl chains. The PP-HDPE/NaMt blend show an important band around 1733 cm^{-1}, relied to the elongation vibrations of C=O group. This band is clearly disappeared by increasing the ZnO content in the nanocomposites, what ever the ZnO content. This result is inagreement with literature.[8,25,26] The Zn O nanoparticles seem to act as a light barrier for the polymer, dut to its superior UV light filtering, leading improve the ultraviolet resistance properties if polymeric materials.

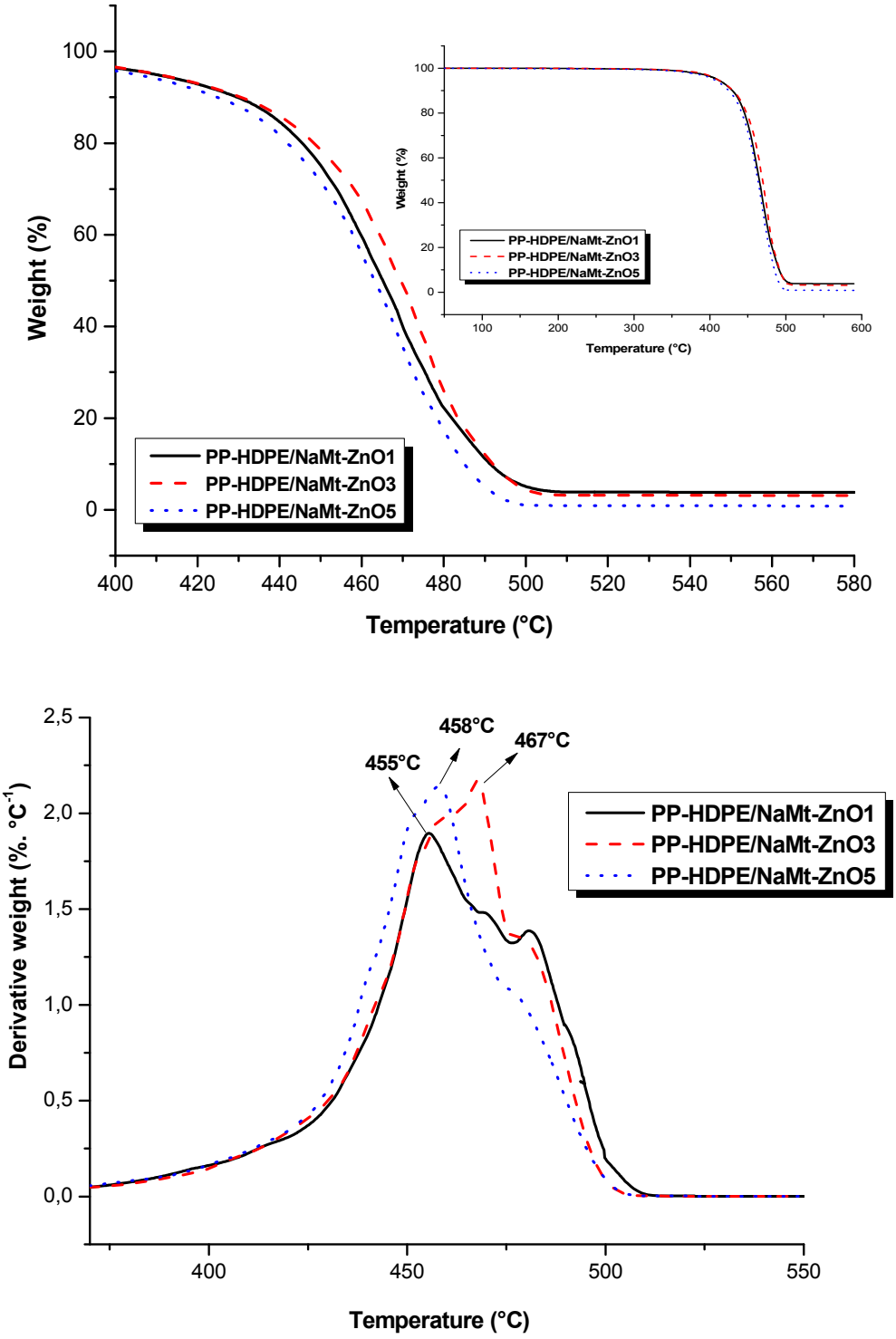

Fig. 5 – TGA/DTG analysis curves of PP-HDPE/NaMt-ZnO nanocomposites, at different NaMt-ZnO content under air, at 20°C min $^{-1}$.

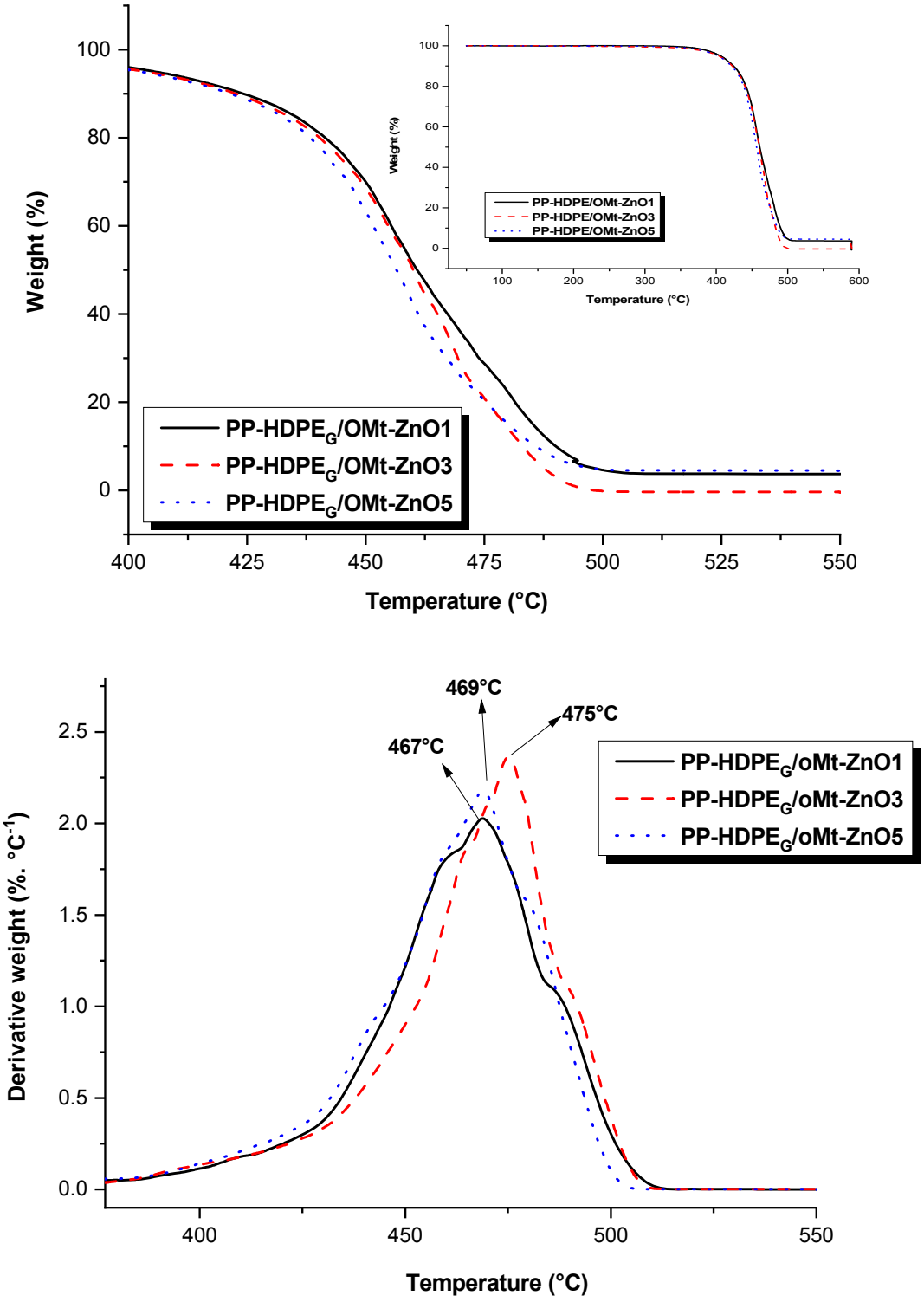

Fig. 6 –TGA/DTG analysis curves of PP-HDPE/oMt-ZnO nanocomposites, at different OMt-ZnO content under air, at 20°Cmin^{-1}.

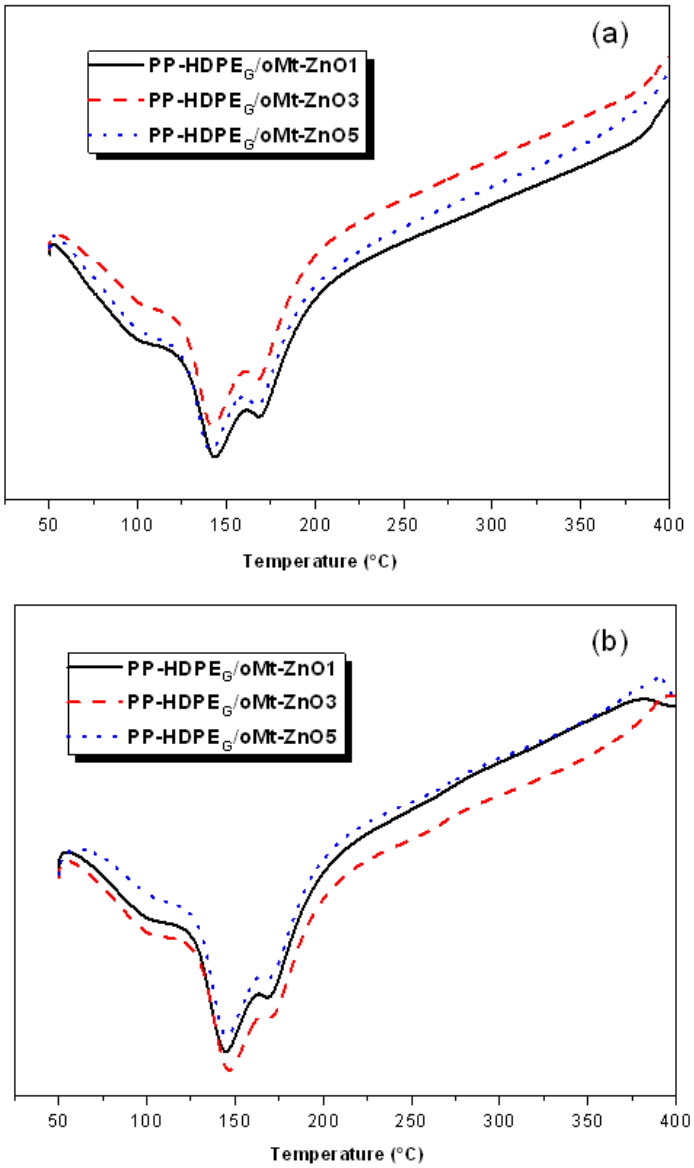

Fig. 7 – DSC analyses of PP-HDPE/NaMt-ZnO (a) and PP-HDPE/oMt-ZnO (b) at different clay-ZnO content. Second heating at 10° C min^{-1}.

Table 2

Antibacterial efficiency of the nanocomposites materials

Material	**(Ct24) (CFU) (×10^5)**	**Log(Ct24) (CFU)**	**Activity**(Log)**	**Standardeviation**
PP-HDPE/NaMt	3.09	5.48	--	--
PP-HDPE /NaMt-ZnO1	1.63	5.21	<1	0.27
PP-HDPE /NaMt-ZnO3	--	--	--	--
PP-HDPE /NaMt-ZnO5	1.36	5.13	<1	0.35
PP-HDPE$_G$/oMt-ZnO1	2.63	5.41	<1	0.07
PP-HDPE$_G$ /oMt-ZnO3	1.09	5.03	<1	0.45
PP-HDPE$_G$ /oMt-ZnO5	1.09	5.03	<1	0.45

Initial Bacteria loading(cfu/mL): Ct24
Logarithmic reduction of grown bacteria colonies (cfu/mL): log(Et),
*Bacteria tested: **Escherichia coli CIP 54 127**, 400 µL of suspension at 2.5 105 cfu/mL
** Activity = log(Ct24) – log(Et), Ct is the reference medium and Et is the medium sample.

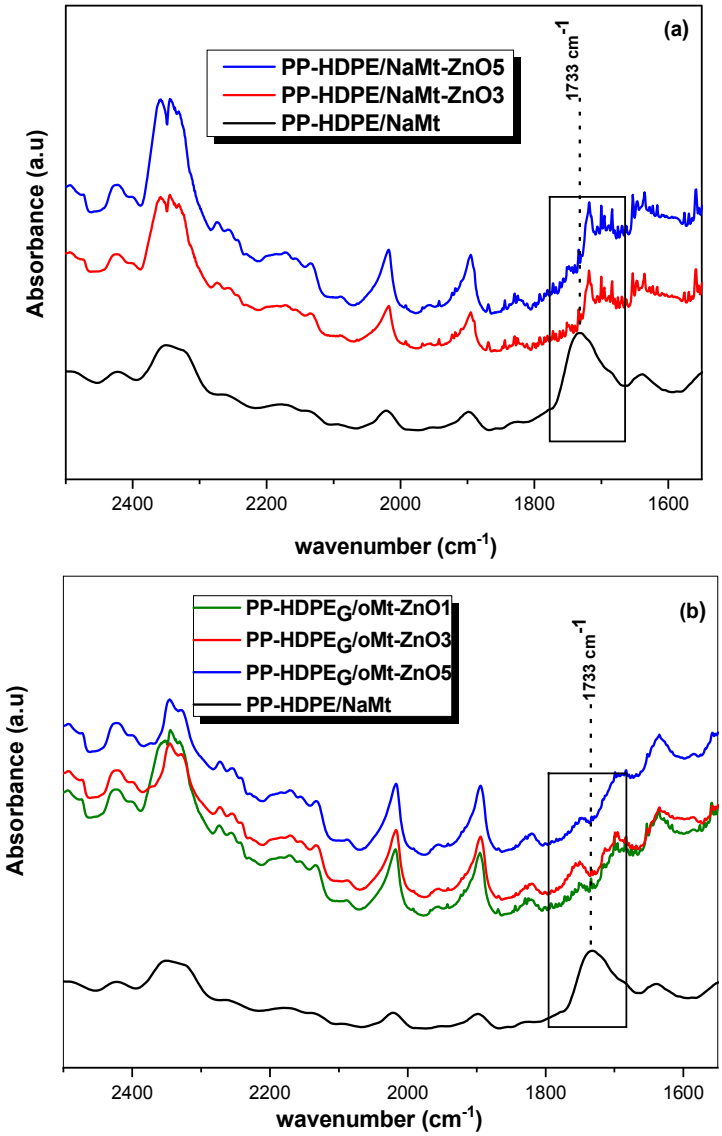

Fig. 8 – FTIR spectra of (a): PP-HDPE/NaMt-ZnO, and (b): PP-HDPE$_G$/oMt-ZnO nanocomposites after 300 h of UV exposure.

5. Antibacterial activity

The antibacterial efficiencies of the nanocomposites materials are shown in Table 2. The initial bacterial loading and survival bacteria after 24h of incubating at 37ºC are given logarithmically. The reduction of the bacteria colonies was calculated by taking the difference between the initial loading and survived bacteria colonies after being counted by spread plate method.[7] The photographs given in Fig. 8 demonstrate the petridishes containing the surviving bacteria colonies in the diluted solution after washing films in sterile 0.9% NaCl solution followed by incubation of 37ºC. In this study, It was seen that the antibacterial efficiencies is present in all the formulations of nanocomposite, and that the addition of ZnO makes appreciably decrease the number of the bacterium. The photographs given in Figure 8 confirm this result, the nanocomposites with highest concentration of ZnO in PP/HDPE$_G$/oMt-ZnO3, PP/HDPE$_G$/oMt-ZnO5 gave the best antibacterial properties as given in Table 2. This result is confirmed by the X-ray mappings. It is noticed that there is no diffraction peak was detected at low 2θ angle, this result is an indication of a total delamination of the clay platelets and hence the formation of exfoliated nanocomposites (Figure 4). The antibacterial mechanism of ZnO is based on photocatalytic activity of the material. During this reaction, generated-OH radicals stick on the membrane of the bacteria and kill them. The attachment and anchoring of ZnO nanoparticles to the surface of modified clay minerals can provide more active surface positions, reduce the agglomeration of nanoparticles and prevent their release into the environment that would result in poor toxicity and would ensure antibacterial activity over time.

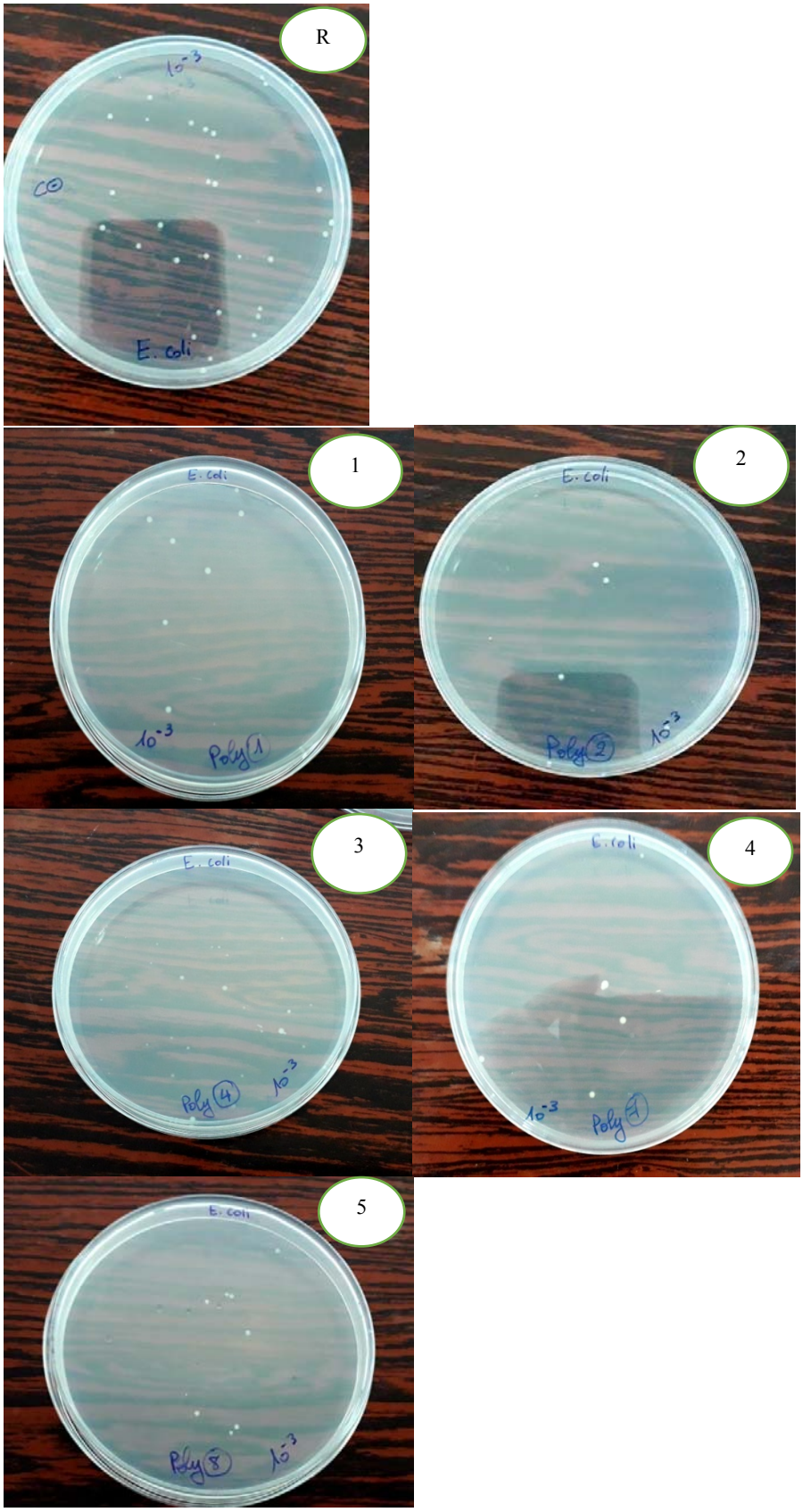

Fig. 9 – Photographs of survival bacteria colonies in diluted solutions corresponds to the cell suspensions obtained after incubation at 37° C; R: control; (1): PP-HDPE/NaMt-ZnO1, (2): PP-HDPE/NaMt-ZnO5, (3): PP/HDPE$_G$/oMt-ZnO1, (4): PP/HDPE$_G$ /oMt-ZnO3, (5): PP/HDPE$_G$ /oMt-ZnO5.

CONCLUSION

Nanocomposites bases on PP-HDPE blend as polymer matrix, clay nanoplatelets and ZnO nanoparticles, as nanofillers were prepared by melt extrusion. The Dynamical arheological analysis DRA results showed that binary blends, as deduced from the torque – time curves exhibit cross-linking reactions. And the evaluation of TB at the equilibrium showed that the crosslinking effect starts to be apparent and given the highest value in the sample (PP/$HDPE_G$/oMt-ZnO5). The XRD results showes the absence of peak at low 2θ angle in the nanocomposite materials PP/$HDPE_G$ /oMt-ZnO1, PP/$HDPE_G$/oMt-ZnO3 and PP/$HDPE_G$ /o-Mt-ZnO5 indicated exfoliated form. The ultraviolet resistance and antimicrobial properties of the obtained nancomposites was made. It is found that the photodegradation of different formulations shown there's no oxidation of the polymers composites in the presence of ZnO. This is due to the superior UV light filtering effects offered by the ZnO particles incorporated into the nanocomposites of PP-HDPE/o-Mt-ZnO5 showed higher antibacterial efficiency against E. coli in well dispersed and hight content of ZnO.

REFERENCES

1. M. Ardusso, A. D. ForeroLópez, N. S. Buzzi, C. V. Spetter and M. D. FernándezSeverin, *Sci. Total Environ.,* **2021**,*763*, 144365.
2. F. Siedenbiedel and J. C. Tiller, *Polym.,* **2012**, *4*, 46–71; doi:10.3390/polym4010046
3. H.Salmi-Mani, G.Terreros, N.Barroca-AubryAymes-Chodur, C.Regeard and P.Roger, *Eur.Polym.J*., **2018**, *103*, 51–58; doi:10.1016/j.eurpolymj.2018.03.038.
4. L. Jérôme, "Greffage de copolymères antibactériens sur des surfaces PVC par chimie Click", *Phd thesis,* Norman Doctoral School of Chemistry INSA in Rouen, Français, **2012**; https://tel.archives-ouvertes.fr/tel-00840218.
5. H. Rokbani, "Elaboration de nouveaux matériaux nanocomposite santibactériens à base de nanoparticules d'oxyde de zinc", *Phd thessis*, Polytechnic School of Montreal, **2018.**
6. A. J. Misra, S. Das and A. P. Habeeb Rahman*, J. Colloid Interface Sci.*, **2018**; doi:https://doi.org/10.1016/j.jcis. 2018.07.020.
7. A. Mirigul and Y. Huseyin, *J. Mater. Sci. Technol.,* **2012**, *28*, 686–692.
8. H. Kouadri, F. Djerbouaa and O. Bouriche, *Rev. Roum. Chim*., **2018**, *63*, 133-142.
9. S. Mustapha, M. M. Ndamitso, A. S. Abdulkareem, J. O. Tijani, D. T. Shuaib, A. O. Ajala and A. K. Mohammed, *Appl. Water Sci*., **2020**, 10-49; https://doi.org/10.1007/ s13201-019-1138-y.
10. S. Kaur, "Synthesis and characterization of ZnO and clay Supported ZnO nanoparticales and their catalytic and antibacterial applications", Master of science in Biochemistry, School of chemistry and biochemistry THAPAR University, PATIALA-147004, **2017**.
11. M. Mizanur Rahman, *Polym.,* **2020**, *12*, 1535. doi:10.3390/polym12071535.
12. E. Tang and S. Dong, *Colloid. Polym. Sci.,* **2009***, 287*, 1025–1032.
13. F. Z. Benabid, N. Kharchi, F. Zouai, A. H. I. Mourad and D. Benachour, *Polym. Polym. Compos*., **2019**, 1-11; https://doi.org/10.1177/0967391119847353.
14. J. Seo, G. Jeon and E. S. Jang, *Applied polymer*., **2011**, 122, 1101-1108; https://doi.org/10.1002/app.34248.
15. D. Ponnammaa, J. J. Cabibihanb, M. Rajanc, S. S. Pethaiah, *Mater.Sci.Eng.B*., **2019**, *98*, 1210-1240.
16. N. J. Hadi, N. A. Saad and D. Alkhfagy, This paper is part of the Proceedings of the 11 International Conferenceth on Engineering Sciences (AFM**2016**) www.witconferences.com Rheological behavior of waste polypropylene reinforced with zinc oxide nanoparticles College of Materials Engineering/Polymer, Babylon University, Iraq.
17. K. B. Deka, K. Tarun, M. Maji, *J. Appl. Polym. Sci*., **2012**, *124*, 2919–2929; doi 10.1002/app.35314 2011.
18. E. D. Lucas-Gil, J. Menéndez, L. Pascual, J. F. Fernándezand F. Rubio-Marcos, *Appl.Sci*., **2020**, *10*, 1322; doi:10.3390/app10041322.
19. D. Gao, Ch. Chen, M. Jianzhong, X. Duan and J. Zhang, *Chem. Eng. J.,* **2014**, 25885.
20. S. Kheiria, M. G. A. Mohameda, M. Amereha, D. Robertsa and K. Kima*, Mater. Sci. Eng*., **2020**, 110754.
21. J. Parameswaranpillai, H. Pulikkalparambil, M. R. Sanjay and S. Siengchin, *Mater. Res. Expr*., **2019**, 6075334.
22. B. Zazoum, E. David, and A. D. Ngo, *Nanocomposites*., **2013**, 1-10; https://doi.org/10.1155/2013/138457.
23. B. Samia, R. Doufnoune, H. Abdelhak, H. Nacceredine C. Esperanza, *J.polym.Eng*., **2013**, *33*, 589– 598; doi 10.1515/polyeng-2013-0048.
24. F. C. Chiu, H. Z. Yen and C. E. Lee, *Poly. Test*., **2010**, *29*, 397; doi:10.1016/j.polymertesting.2010.01.004.
25. Q. Huaili, Z. Shimin, L. Huiju, X. Shaobo, Y. Mingshu and S. Deyan, *Poly*., **2005**, *46*, 3149; doi:10.1016/ j.polymer.2005.01.087
26. M. Sandrine, M. Bénédicte, G. David and G. Jean-Luc, *Chem. Mater*., **2004**, *16*, 377; doi:10.1021/cm031079k.
27. S. Bouhelal, M. E. Cagiao, M. L. D. Lorenzo, F. Zouai, S. Khellaf, H. Tabet and Dj. Benachour, *J. Polym. Eng*., **2012**, *32*, 143 ; doi 10.1515/polyeng-2011-0130.